Barrier Properties in Hydrogenated Acrylonitrile Butadiene Rubber Compounds Containing Organoclays and Perfluoropolyether Additives

Roberto Valsecchi,[1] Luca Torlaj,[2] Stefano Turri,[2] Claudio Tonelli,[1] Marinella Levi[2]

[1]*Solvay Solexis, Viale Lombardia 20, 20021 Bollate (Milano), Italy*
[2]*Dipartimento di Chimica, Materiali e Ingegneria Chimica "Giulio Natta," Politecnico di Milano, Piazza Leonardo da Vinci 32, 20133 Milan, Italy*

Received 16 February 2010; accepted 23 June 2010
DOI 10.1002/app.32995
Published online 29 September 2010 in Wiley Online Library (wileyonlinelibrary.com).

ABSTRACT: Elastomeric compounds from hydrogenated acrylonitrile butadiene rubber, organomodified clay, and perfluoropolyether (PFPE) additives were prepared. Characterization of the materials included X-ray diffraction, dynamic mechanical analysis (DMA), tensile mechanical properties testing, environmental scanning electron microscopy, and solvent permeability measurements, from which the solubility coefficient (*S*) and diffusion coefficient (*D*) values were determined. A synergistic effect of the two additives was observed because the presence of clay reduced *D*, whereas PFPE mainly decreased *S*. Increasing the mixing time facilitated the dispersion of the clay layers. DMA and the diffusivity data were used to estimate the aspect ratios of the solid inclusions in the rubber. © 2010 Wiley Periodicals, Inc. J Appl Polym Sci 119: 3476–3482, 2011

Key words: clay; diffusion; elastomers; fluoropolymers

INTRODUCTION

Fluoroelastomers[1] are often used for manufacturing gaskets, O-rings, and packers in oil-well completion and production because of their outstanding chemical resistance to oil and solvents. These materials are proposed when rubberlike elasticity is needed in severe environments. However, the high cost of fluoroelastomers makes the use of these materials prohibitive in many applications. Attempts to provide less expensive compositions with performances that approach those of fluoroelastomers have been made. Among nonfluorinated elastomers, hydrogenated acrylonitrile butadiene rubber (HNBR) represents a specialty rubber with good thermal, oil, UV, and ozone resistance. To further improve its chemical resistance, several efforts have been made in the past; for example, the blending of hydrogenated rubbers with fluoroelastomers is a common practice.[2] More recently, the compounding of nitrile rubbers with organoclays has been suggested as a method for enhancing the rubber performance[3–6] because the dispersion of inorganic platelets can, in principle, greatly increase the tortuosity of the path that diffusing molecules must follow during the permeation through the polymeric membrane. This reduces the diffusion coefficient or diffusivity (*D*) and, therefore, increases the overall chemical resistance. In this study, the effect of the introduction of organomodified layered silicates and high-molecular-weight perfluoropolyether (PFPE) additives on the properties of HNBR compounds was studied.

Correspondence to: S. Turri (stefano.turri@polimi.it).

Journal of Applied Polymer Science, Vol. 119, 3476–3482 (2011)

EXPERIMENTAL

Materials

HNBR (Zetpol2000) having a 36.2% acrylonitrile content and 1% residual double bonds was provided by Zeon Chemicals, Niederkasseler, Germany. This rubber exhibited a Mooney viscosity of ML (1 + 4) 100°C of 85. Montmorillonite organically modified with methyl tallow bis(2-hydroxyethyl) quaternary ammonium chloride [Cloisite30B (CL30B)] was purchased from Southern Clays, Austin, Texas. The interlayer distance of this organoclay was 1.82 nm.

An amorphous, high-molecular-weight PFPE–polyamide polymer (Fluorolink PA100E PFPE, Solvay-Solexis, Bollate, Italy) was used as additive. Its chemical structure[7] is illustrated as follows:

$$[HN(CH_2)_6HNCOCF_2O(CF_2CF_2O)_p(CF_2O)_qCF_2CO]_n-$$

Some characteristics are summarized in Table I. Dicumyl peroxide (DCPO) with 40% active compound (LuperoxDC40KEP) and triallyl isocyanurate (TAIC; 75% on silica carrier) were supplied by Sigma-Aldrich, Milan, Italy.

TABLE I
Characteristics of the PA100E PFPE Additives

p/q	M_w (g/mol)	M of PFPE block (g/mol)	%F (w/w)	T_g (°C)	δ $(MPa)^{0.5}$ [a]
1.8–2.0	10,000–30,000	1500 ± 100	57.4	−85	16.2

M_w = weight-average molecular weight; p/q = compositive ratio, M = molecular weight, %F = weight percentage of fluorine, δ = solubility parameter.
[a] Calculated according to the group contribution method[11] by assignment of a value of 11 $MPa^{0.5}$ for PFPE segment.[12]

Preparation of the HNBR/organoclay/PFPE compounds

HNBR compounds were prepared by a melt-mixing method with an internal mixer Plasticorder W 50 EHT (Brabender, Duisburg, Germany) operating at 20 rpm. During mixing, the temperature was kept below 100°C with external cooling. The rubber was first added to the kneader, and after the torque reached a constant value, both the CL30B clay (3 and 6 phr) and fluorinated additive (10–30 phr) were gradually added too. The compound was mixed for 1 h, after which DCPO (5 phr, 2 phr of active compound) and TAIC (4 phr, 3 phr of active chemical) were added. In some cases, the mixing time was extended up to 3 h to study its effect on the properties of the final material. The rubber compounds were then cured at 170°C in an electrically heated hydraulic press; the curing cycle was determined by dynamic mechanical analysis (DMA; isothermal testing at constant frequency of 1 Hz) as the time needed to reach a constant storage modulus (G') value and was typically around 20 min. Table II describes the formulation of the final compounds prepared: the amount of clay and PFPE additive present are specified by the numbers after the letters C and P, respectively. The mixing time (1 or 3 h) is also specified.

Characterization of the compounds

DMA was carried out with a Mettler Toledo DMA/SDTA 861[e] instrument (Mettler Toledo, Im Langacher, Switzerland) in shear sandwich mode at constant frequency of 1 Hz and a strain of 0.25% in heating runs from −100 to 100°C (speed = 2°/min).

The state of dispersion of the organoclay in the rubber vulcanizate was investigated by X-ray diffraction (XRD). XRD patterns were obtained with a Philips PW 1710 diffractometer (PANalytical, Almelo, the Netherlands) with Cu Kα radiation (λ = 0.15406 nm). The range of 2θ scans was 2–15°. The basal spacing (d) of the clay was estimated from the (001) peak in the XRD pattern according to the Bragg's law:

$$n\lambda = 2d_{nhnknl} \sin\theta \quad (1)$$

n is an integer, λ is the wavelength of incident light, d_{nknhnl} is the interplanar spacing, θ is the angle between the incident light and the scattering planes.

A Zeiss EVO 50 variable-pressure environmental scanning electron microscope (Zeiss, Oberkochen, Germany) operating at 20 kV and 250 pA was used to characterize the morphology of the compounds. Fractured compound surfaces were observed under both secondary electron and backscattering modes. X-ray microanalysis was also carried out with an Oxford INCA Energy 200 EDS system (Oxford Instruments, Abingdon, UK).

The transport properties were measured by sorption experiments in toluene at 23 ± 2°C. Rubber samples (20 × 20 × 1 mm^3) were swollen in solvent and, after a gentle surface drying, weighed at periodic intervals until a constant weight value (equilibrium) was reached. The samples were then deswollen to a constant mass by heating *in vacuo* (10^{-1} mmHg) at 50°C. The solubility coefficient (S) was then calculated through the following equation:

TABLE II
Compositions of the Prepared Compounds

Component/compound	H	H-C3 1 h	H-C6 1 h	H-C3P30 1 h	H-C6P30 1 h (3 h)	H-C6P10 3 h	H-C6P20 3 h
HNBR (Zetpol2000)	100	100	100	100	100	100	100
DCPO	5 (2[a])	5 (2)	5 (2)	5 (2)	5 (2)	5 (2)	5 (2)
TAIC	4 (3[a])	4 (3)	4 (3)	4 (3)	4 (3)	4 (3)	4 (3)
CL30B	—	3	6	3	6	6	6
Fluorolink PA100E PFPE	—	—	—	30	30	10	20

The time of mixing is indicated after the name of each compound.
[a] Active compound content.

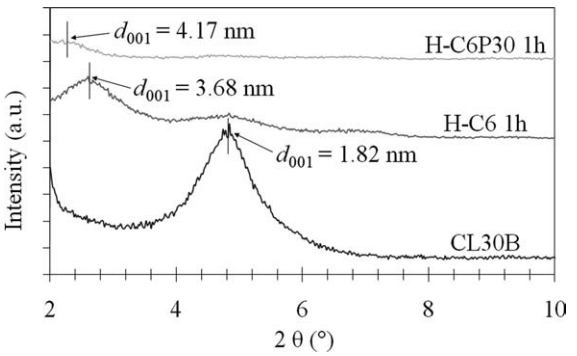

Figure 1 XRD spectra of H-C6 1 h and H-C6P30 1 h compared to that of pristine clay.

$$S = \frac{m_\infty - m_0}{m_0} \quad (2)$$

where m_∞ is the equilibrium mass of the swollen samples and m_0 is the mass after deswelling.

D was calculated with the time-lag method[8] according to eq. (3) and with the weighting cup procedure (see ASTM D 814):

$$\tau = \frac{l^2}{6D} \quad (3)$$

where l is the rubber membrane thickness and τ is the time lag for diffusion, that is, the time after which the system reaches a steady state or a constant flux state.

The permeability coefficient or permeability (P) was calculated as the product of S and D.

The tensile stress–strain properties were determined with a Hounsfield dynamometer at an extension rate of 100 mm/min at room temperature according to ASTM D 412 (Hounsfield, Salfords, UK).

RESULTS AND DISCUSSION

XRD pattern

Figure 1 shows the XRD patterns for the H-C6 1 h and H-C6P30 1 h compounds in comparison to the pristine CL30B clay. The spectrum of CL30B exhibited a typical reflection at $2\theta = 4.86°$, which corresponded to a d_{001} of 1.82 nm according to Bragg's law. After compounding, the interlayer spacing of the clay increased from 1.82 to 3.68 and 4.17 nm for H-C6 1 h and H-C6P30 1 h, respectively; this suggested the formation of intercalated nanostructures. Nevertheless, the 001 peak was extremely weak, possibly because of a lack of order caused by hydrogen-bonding interactions among the hydroxyethyl groups of the CL30B surfactant and the acrylonitrile CN groups of the HNBR. This was particularly true in the case of H-C6P30 1 h, where first-order peak was broader and lower in intensity and the second- and third-order peaks practically disappeared. The effect of the fluorinated additive is also shown in Figure 2, where the XRD patterns of H-C6P10 3 h, H-C6P20 3 h, and H-C6P30 3 h are compared. With increasing amount of PFPE additive from 10 to 30 phr, the peak intensities decreased, and the interlayer spacing remained substantially the same. Therefore, the presence of fluorinated additive seemed to have only a minor effect on the clay dispersion. As shown in Figure 2, in all cases, second- and third-order peaks are still visible.

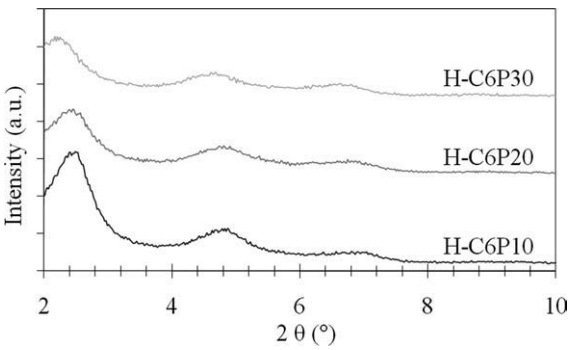

Figure 2 XRD spectra of H-C6P10 3 h, H-C6P20 3 h, and H-C6P30 3 h.

Environmental scanning electron microscopy (ESEM)

To study clay and additive distribution and compound morphology, ESEM analyses were carried out

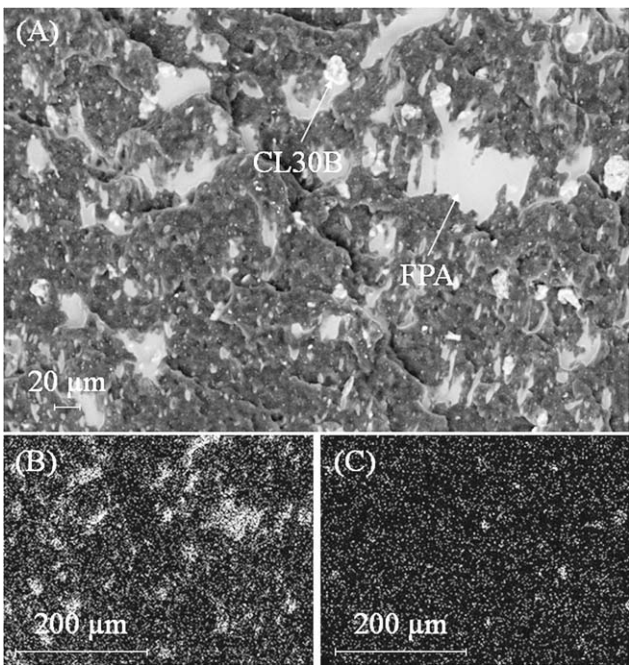

Figure 3 Backscattering image of the cross sections of (A) H-C6P30 1 h with its respective (B) fluorine and (C) silicon elemental maps. FPA means fluorinated polyamide.

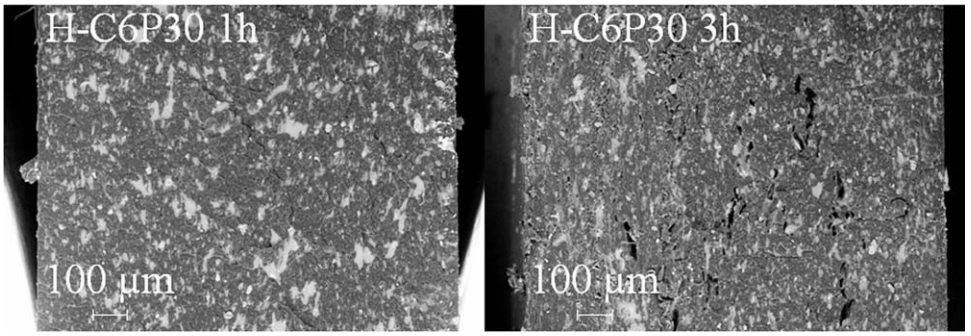

Figure 4 Backscattering images for H-C6P30 1 h (left) and H-C6P30 3 h (right).

on the fractured surfaces of vulcanized slabs. Figure 3(A) shows the backscattering image of H-C6P30 1 h, in which different phases—rubber, clay, and PFPE—were easily distinguishable because of the differences in atomic number between carbon, silicon, and fluorine; this provided a clear color contrast. The brighter regions were, therefore, attributed to the presence of clay platelets uniformly distributed in the polymeric matrix. The corresponding F and Si elemental maps are actually shown in Figure 3(B,C), which gives clear information on the phase distributions. The influence of the mixing time on the CL30B and PFPE dispersion and distribution is shown in Figure 4, which compares the backscattering ESEM images of the H-C6P30 1 h and H-C6P30 3 h vulcanizates. With increasing mixing times from 1 to 3 h, the average dimensions of the PFPE domains decreased and were better distributed within the elastomeric matrix.

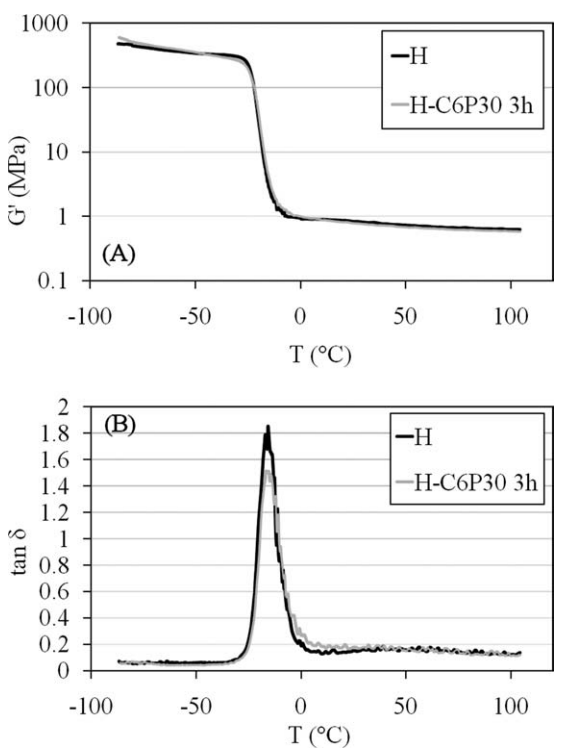

Figure 5 Temperature dependence of (A) G' and (B) tan δ for H and H-C6P30 3 h.

Mechanical properties

In rubber compounds, the elastic modulus depends on the filler content and filler aspect ratio (f).[9] The modulus in the rubbery plateau can be described by Guth's equation[10]:

$$G'_c = G'_m\left(1 + 0.67f\phi + 1.62f^2\phi^2\right) \quad (4)$$

where G'_c and G'_m are the storage moduli of the composite and the polymer matrix, respectively, and ϕ is the volume fraction of the filler. The reference unfilled polymer should have been, in our case, a rubber compound that contained the corresponding amount of fluorinated additive. A sample DMA curve is shown in Figure 5, from which G' values in the rubbery plateau were obtained. The numerical results of the data fitting are reported in Table III. The small value of f found suggested the presence of aggregated and intercalated clay structures, as already observed both in the XRD and ESEM analysis. No substantial variation in f was observed with both increasing mixing time and the addition of different amounts of fluorinated additive.

The high-temperature plateau modulus [$G(T)$], well above any other thermal relaxation process, can be used also to estimate the density of crosslinking

TABLE III
Average f Values of the Clay Layers, Crosslink Density, and Its Contributions

Sample	f_{Guth}	v (mol/m^3)	v_r (mol/m^3)	v_f (mol/m^3)
H	—	200	200	—
H-C3 1 h	11	226	220	6
H-C6 1 h	10	254	241	13
H-C3P30 1 h	1	161	157	3
H-C6P30 1 h	12	206	197	9
H-C6P10 3 h	15	242	231	12
H-C6P20 3 h	10	235	224	10
H-C6P30 3 h	9	191	183	8

TABLE IV
Mechanical Properties from the Tensile Tests at Room Temperature

Sample	Ultimate strength (MPa)	Elongation at break (%)	Modulus at 100% elongation (MPa)
H	3.70 ± 0.35	4.91 ± 0.45	0.75 ± 0.02
H-C3 1 h	5.18 ± 0.19	5.35 ± 0.31	0.95 ± 0.05
H-C6 1 h	6.38 ± 0.43	3.67 ± 0.38	1.67 ± 0.04
H-C3P30 1 h	3.14 ± 0.36	3.77± 0.39	0.79 ± 0.08
H-C6P30 1 h	3.24 ± 0.30	3.45 ± 0.42	0.96 ± 0.04
H-C6P10 3 h	5.92 ± 0.19	4.09 ± 0.29	1.37 ± 0.04
H-C6P20 3 h	6.37 ± 0.24	4.01 ± 0.28	1.32 ± 0.06
H-C6P30 3 h	5.43 ± 0.36	4.08 ± 0.35	1.10 ± 0.08

(v) of vulcanized rubbers according to the classical rubber elasticity theory[11]:

$$v = \frac{G(T)}{RT} \tag{5}$$

where R is the universal gas constant; T, temperature. The v values obtained from the G' measurements at 100°C are summarized in Table III.

According to Bueche's[12] theory and eq. (6), the separated crosslinking density contributions of the rubber network (v_r) and the filler (v_f) to the effective v are also reported in Table III (where σ is the stress and λ is the elongation):

$$\sigma = (v_r + v_f)RT\left(\lambda - \frac{1}{\lambda^2}\right) \tag{6}$$

We observed that the introduction of the clay increased the overall apparent v of the rubber, but the values of v_f were very small; this suggested poor interaction between the rubber and the organomodified clay. It seemed that the mixing time (passing from 1 to 3 h) slightly improved f and the apparent v of the compounds, whereas PFPE progressive loading had an opposite effect.

The effects of clay and the fluorinated additive on the tensile mechanical properties of HNBR compounds were studied, and the results are summarized in Table IV. In the absence of PFPE, both the tensile modulus and strength were significantly increased by the presence of the clay (+40% and over +70% for H-C3 1 h and H-C6 1 h, respectively). With the introduction of the low-glass-transition-temperature (T_g) fluorinated additive, the modulus and strength decreased very slightly, but they still remained comparable with that of neat HNBR; this confirmed the DMA data (Fig. 5). The modulus increased again with increasing mixing time from 1 to 3 h; this was probably due to an improved interaction between HNBR and CL30B.

Sorption and barrier properties

The study of the P behavior with hydrocarbon solvent is of great interest for applications and can give indirect information about the material morphology. D and S were separate contributors to P, which was defined as $P = DS$. The effects of the clay particles and PFPE additive on D and S were studied separately, as explained in the Experimental section. The barrier properties of the HNBR rubber/organoclay/PFPE compounds are summarized in Table V. As far as the D values are concerned, Figure 6 shows, as an example, the time-lag curve for the permeation of toluene through the H-C3P30 1 h membrane at room temperature. The intercept of the linear part of the curve with the time axis is referred to as the *lag time*, from which the D's could be calculated according to eq. (3), as described in the Experimental section. For the HNBR/CL30B rubber nanocomposites (H-C3 1 h and HC6 1 h compounds), a clear

TABLE V
P, S, and D Values of Different HNBR/CL30B/Fluorolink PA100E PFPE Compounds at 23°C

Sample	S	$D \times 10^7$ (cm^2/s)	$P \times 10^7$ (cm^2/s)
H	1.97 ± 0.07	6.02 ± 0.08	11.86
H-C3 1 h	1.95 ± 0.11	5.58 ± 0.07	10.88
H-C6 1 h	1.91 ± 0.09	5.27 ± 0.12	10.07
H-C3P30 1 h	1.64 ± 0.05	5.60 ± 0.14	9.18
H-C6P30 1 h	1.58 ± 0.08	5.51 ± 0.11	8.71
H-C6P10 3 h	1.49 ± 0.10	5.01 ± 0.08	7.46
H-C6P20 3 h	1.38 ± 0.05	4.87 ± 0.06	6.72
H-C6P30 3 h	1.31 ± 0.09	4.71 ± 0.09	6.17

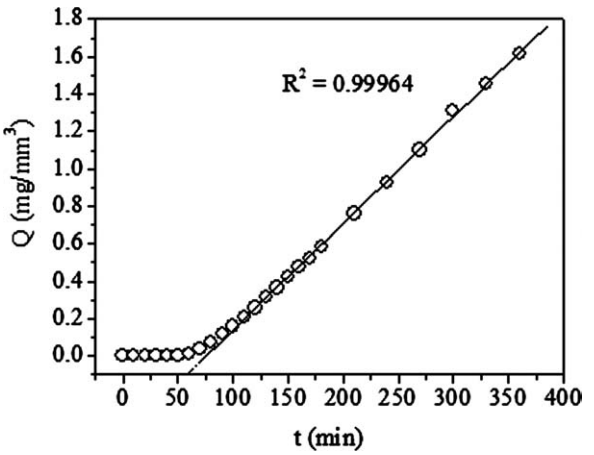

Figure 6 Time-lag curve for the diffusion of toluene through H-C3P30 1 h membrane at room temperature. Q, normalized amount of solvent transmitted through the membrane; t, time.

reduction in D was observed. The behavior was attributed to the tortuosity created by the dispersed clay platelets. However, the decrease in D seemed quite small; this confirmed the presence of predominantly intercalated structures with a minimal degree of exfoliation. The segregated particles of the PFPE additives also may have acted as barrier materials because they were intrinsically repellant toward hydrocarbons. However, when we compared the H-C3 1 h and HC6 1 h compounds with the H-C3P30 1 h and HC6P30 1 h products, a slight increase in D was observed. This could have been because the minimal fraction of solvent miscible with the PFPE additive could diffuse through a phase having a quite large free volume because of the very low T_g of the PFPEs (ca. -100°C). However, when the contents of clay and PFPE were kept at 6 and 30 phr, respectively, and with increasing mixing time from 1 to 3 h, D decreased from 5.51 to 4.71 cm^2/s, probably because of an increase in the tortuosity caused by the clay.

The S values are reported in Table V, too. Compared with neat HNBR (sample H), a remarkable decrease in S was observed only in the presence of the PFPE additive. This reduction was due to the mutual thermodynamic immiscibility between toluene and PFPE (the difference between S parameters[13,14] was $\Delta\delta = 18.2–16.2 = 2.0$ $MPa^{0.5}$). A progressive reduction in S was observed with increasing mixing time and increasing amount of additive from 10 to 30 phr. On the basis of the combination of S and the diffusion behavior, the average P showed a remarkable reduction, which was particularly evident in the case of compounds containing higher amounts of both CL30B and PFPE. For example, the P reduction was as high as 48% for the H-C6P30 3 h compound. This may have been due to the synergistic action of CL30B and Fluorolink PA100E PFPE in reducing D and S respectively.

A quantitative modeling of the diffusivity behavior was made to estimate, in an alternative way, f of the clay inclusions. The classical Nielsen model[15] is based on a two-dimensional diffusion through a membrane containing infinitely long, rectangular cross-section plates uniformly dispersed in the polymer and placed normally to the direction of mass transfer. Through calculation of the maximum tortuosity factor, the largest possible ratio of the diffusivity of a molecule through a neat polymer (D_0) to that of the same molecule through the filled polymer (D) is given by

$$\frac{D_0}{D} = 1 + \frac{f\phi}{2} \tag{7}$$

More recently, Cussler et al.[16–19] studied the diffusion problem through flake-filled membranes and developed an extensive theory for predicting the change in diffusivity as a function of the loading level and f; this led to a slightly different equation:

$$\frac{D_0}{D} = 1 + \frac{f^2\phi^2}{1-\phi} \tag{8}$$

The f value of the clays was estimated from the experimental diffusivity data according to eqs. (7) and (8), and the numerical results are shown in Table VI. The values found were in substantial agreement with those from the dynamic mechanical data (see Table IV).

CONCLUSIONS

Elastomeric compounds from HNBR, organoclay, and PFPE additive were successfully prepared by a melt-mixing technique. The small f values of clay inclusions (from both DMA and diffusivity data) suggested the presence of aggregates and intercalated structures, as also evidenced by both XRD and ESEM analyses. In the absence of the PFPE additive, both the tensile modulus and mechanical strength of the vulcanizates were significantly increased in the presence of the clay, whereas the low-T_g fluorinated additive had a very minor effect on the tensile properties. The P values were reduced, especially in the case of longer mixing times and with compounds containing higher amounts of both the organoclay

TABLE VI
Average f Values of the Clay Layers from D Studies

Sample	$f_{Nielsen}$	$f_{Cussler}$
H-C3 1 h	12	21
H-C6 1 h	11	14
H-C3P30 1 h	10	21
H-C6P30 1 h	7	12
H-C6P10 3 h	22	21
H-C6P20 3 h	15	18
H-C6P30 3 h	22	22

and fluorinated PFPE additive. This could have been due to the synergistic action of the organoclay and fluorinated additive in reducing *D* and *S*, respectively. Applicative results could be significantly improved by a more efficient dispersion and delamination of clays in the rubber.

References

1. Ameduri, B.; Boutevin, B.; Kostov, G. Prog Polym Sci 2001, 26, 105.
2. Hirano, K.; Suzuki, K.; Nakano, K.; Tosaka, M. J Appl Polym Sci 2005, 95, 149.
3. Kim, J. T.; Oh, T. S.; Lee, D. H. Polym Int 2003, 52, 1203.
4. Nah, C.; Ryu, H. J.; Kim, W. D.; Chang, Y. W. Polym Int 2003, 52, 1359.
5. Gatos, K. G.; Sawanis, N. S.; Apostolov, A. A.; Thomann, R.; Karger-Kocsis, J. Macromol Mater Eng 2004, 289, 1079.
6. Gatos, K. G.; Karger-Kocsis, J. Eur Polym J 2007, 43, 1097.
7. Tonelli, C.; Gavezotti, P.; Strepparola, E. J Fluor Chem 1999, 95, 51, and references therein.
8. Comyn, J. In Polymer Permeability; Elsevier Applied Science: New York, 1988.
9. Ke, Y. C.; Long, C. F.; Qi, Z. N. J Appl Polym Sci 1999, 71, 1139.
10. Guth, E. Proceedings of the Second Rubber Technology Conference, London, W. Heifer & Sons, Ed., Cambridge (UK) 1948; p 353.
11. Treloar, L. R. G. In The Physics of Rubber Elasticity; Clarendon: Oxford, 1975.
12. Bueche, F. In Reinforcement of Elastomers; Kraus, G., Ed.; Interscience: New York, 1965.
13. Van Krevelen, D. W. In Properties of Polymers; Elsevier: Amsterdam, 1976.
14. Marchionni, G.; Ajroldi, G.; Righetti, M. C.; Pezzin, G. Macromolecules 1993, 26, 1751.
15. Nielsen, L. E. J Macromol Sci Chem 1967, 1, 929.
16. Cussler, E. L.; Hughes, S. E.; Ward, W. J., III; Aris, R. J Membr Sci 1988, 38, 161.
17. Eitzman, D. M.; Melkote, R. R.; Cussler, E. L. AIChE J 1996, 119, 129.
18. Yang, C. F.; Nuxoll, E. E.; Cussler, E. L. AIChE J 2001, 47, 295.
19. Moggridge, G. D.; Lape, N. K.; Yang, C. F.; Cussler, E. L. Prog Org Coat 2003, 46, 231.